Review

Intensity Correlation Imaging and Nonnegative Dynamic Systems

David Hyland *

Posted Date: 14 February 2025

doi: 10.20944/preprints202502.1067.v1

Keywords: Hanbury Brown and Twiss effect; Two-dimensional imaging; Integration time reduction; Noise reducing phase retrieval; Stochastic search algorithm; Phase retrieval algorithms; Cramér-Rao bound; Nonnegative dynamic systems

Review

Intensity Correlation Imaging and Nonnegative Dynamic Systems

David Charles Hyland

Professor Emeritus, Texas A&M University, College Station, Texas, and Independent Researcher, 1913 Sherrill Court, College Station, 77845 Texas, USA; al1kuddaula@gmail.com#

Abstract: This work is a supplement to the the author's "The Rise of the Brown-Twiss Effect" featured in the Photonics special issue: "Optical Imaging and Measurements: 2nd Edition". The main contribution for the author's algorithm was the survey of the stochastic search algorithm required to determine the true noise free-image via the Brown-Twiss effect with enormously small integration times. A key element in the algorithm was the introduction of initial conditions where the values of the intensity pixels are assumed to be mutually statistically independent and uniformly distributed over the range $[0,\delta)$ where δ is a (very small) positive constant. This algorithm performed quite well, but the small initial conditions are unnecessary, as well as other complications that should be simplified. Here we streamline the algorithm in the form of a discrete-time dynamic system and explore the alternate features and benefites of compartmental nonnegative dynamic systems.

Keywords: Hanbury Brown and Twiss effect; two-dimensional imaging; integration time reduction; noise reducing phase retrieval; stochastic search algorithm; phase retrieval algorithms; Cramér-Rao bound; nonnegative dynamic systems

---

1. Introduction

Recent work of the present Author has succeeded in the vast reduction of integration times that have so long plagued the Hanbury Brown-Twiss effect. The way is now open to reap the advantages of simple, inexpensive flux collecting hardware, immunity to seeing conditions, and unlimited baselines and image resolution. Furthermore since the Brown- Twiss effect has been extended to two-dimensional imaging; it is appropriate that we term the algorithm the Intensity Correlation Imaging (ICI) algorithm.

Within the "The Rise of the Brown-Twiss Effect" surveyed in this special issue the reduction of integration times has been accomplished by means of the Noise Reducing Phase Retrieval (NRPR) algorithm which is embedded within a Stochastic Search algorithm. In the complex analysis of [1], initial conditions, such as small random perturbations in the pixel intensities and other complexities, the algorithm performed very well. However, in this paper we update and simplify the algorithm by constructing a discrete-time dynamic system. Moreover, not only does the algorithm perform as well as the original, but we also introduce the benefits of a nonnegative dynamic systems.

We progress as follows. Section 2 begins with the NRPR algorithm, which contains the correct integration times and sets up the foreground/background dichotomy. Section 3 transforms the NRPR steps into a discrete-time, nonnegative dynamic system. Section 4 merges the dynamic system within the Stochastic search algorithm structured to gradually reduce the "Box" sizes.

2. Description of the NRPR Algorithm

It is supposed that there is an array of flux collecting apertures arranged so as to form a square, evenly spaced grid on the "u-v plane" (which, in interferometry, denotes the Fourier domain projected on the plane perpendicular to the target line-of-sight). The grid has a one-to-one

 doi:10.20944/preprints202502.1067.v1

correspondemce to a matrix of $N \times N$ pixels forming the construction of an image of a luminous object amidst a black sky. The defining characteristics of the NRPR algorithm are:

$g \in \mathrm{C}^{N\times N}$ = Current value of the estimated image (pixellated)

$\overline{g} \in \mathrm{R}^{N\times N}$ = The true image, without noise

$\tau \in \mathrm{R}^{N\times N}$ = Unity for for pixels constrained to have zero intensity and zeros for pixels that are unconstrained

$\tau_{\perp} \in \mathrm{R}^{N\times N} = I_{N\times N} - \tau$, The opposite of τ

$\Im[...]$ = Two-dimensional Fast Fourier Transform (unitary)

$\overline{G} = \Im[\overline{g}] \in \mathrm{C}^{N\times N}$ = The true coherence, without noise

$\hat{\mathrm{G}} \in \mathrm{R}^{N\times N}$ = The measured coherence magnitude obtained by cross-correlating the intensity signals from all pairs of the flux collecting apertures

$(\Im[g])_{kj}$ = FFT in the u-v plane. $(\Im[g])_{kj} = (\Im[g])^{*}_{jk}$

$\mathrm{Re}[...] \triangleq \frac{1}{2}\left([...]+[...]^{*}\right)$, The real valued portion of $[...]$

$\mathrm{Re}_{+}[...] \triangleq \max\left\{0, \frac{1}{2}\left([...]+[...]^{*}\right)\right\}$, The real positive value of $[...]$ (1. a-k)

$(A)\circ(B) \triangleq$ Hadamard product of A and B

The matrix τ defines the set of constraints. $\tau_{kj} = 1$ declares pixel (k, j) to be constrained to be zero, whereas $\tau_{kj} = 1$ if g_{kj} is unconstrained. Matrix $(\tau_{\perp})_{kj}$ is the opposite; unity for uncnstrained pixels and zero for constrained pixels. The region wherein $\tau_{kj} = 1$ we have termed "the background", and the remaining region, "the foreground". In this scenario, the initial inputs and the subsequent algorithm are defined as in Figure 2.

Figure 2 shows the various steps of the NRPR algorithm. There are several initial specifications. The first is the measured coherence magnitude, $\hat{G}(\mathbf{u}_k, \Delta T) = \left|\gamma(\mathbf{u}_k)\right|^2 + \frac{N_C}{4\sqrt{2}}\left|\gamma_{est}\right|^2 N_{\mathbf{u}_k}(0,1)\Big|^{1/2}$ which obeys a positivity constraint. This is composed of the noise-free normalized coherence magnitude, $\left|\gamma(\mathbf{u}_k)\right|$, where $\mathbf{u}_k$ is the relative position vector of a pair of the flux collecting apertures, $N_{\mathbf{u}_k}(0,1)$ is a complex-valued Gaussian noise of zero mean and unit variance and N_C is the number of constrained pixels, i.e. $N_C = \sum_{k=1}^{N}\sum_{j=1}^{N}\tau_{kj}$. The formulation of this noise model was accomplished in [2] resulting in an asymptotic expression for the precision estimate of the necessary integration time. The second initial specification is $g = g_0$ where g_0 is independently and uniformly distributed in $(0, \delta]$ where δ is real and positive. It is these random specifications of the initial values of the pixel intensities that we wish to supplant with a dynamic system having additional simplifications.

It must be emphasized that only a single data batch of measured coherence magnitude measurements will be used in the process by which the zero-noise image is determined. Thus the adaptive algorithms described here do not increase the necessary integration time. However, the adaptive algorithms require repeated NRPR computations, and each such repetition uses a new seed for the randomized initial guess for the image.

The various steps *A* to *F* of the algorithm are discussed in References [1–3]. The basic computations of NRPR are directed to an *hypothesis* that a square "box" of size B_x and, positioned in the center of the field of view, contains the noise-free image. Then NRPR is embedded within the Stochastic Search wherein the hypothesis is *tested* and the noise-free image is discovered.

 doi:10.20944/preprints202502.1067.v1

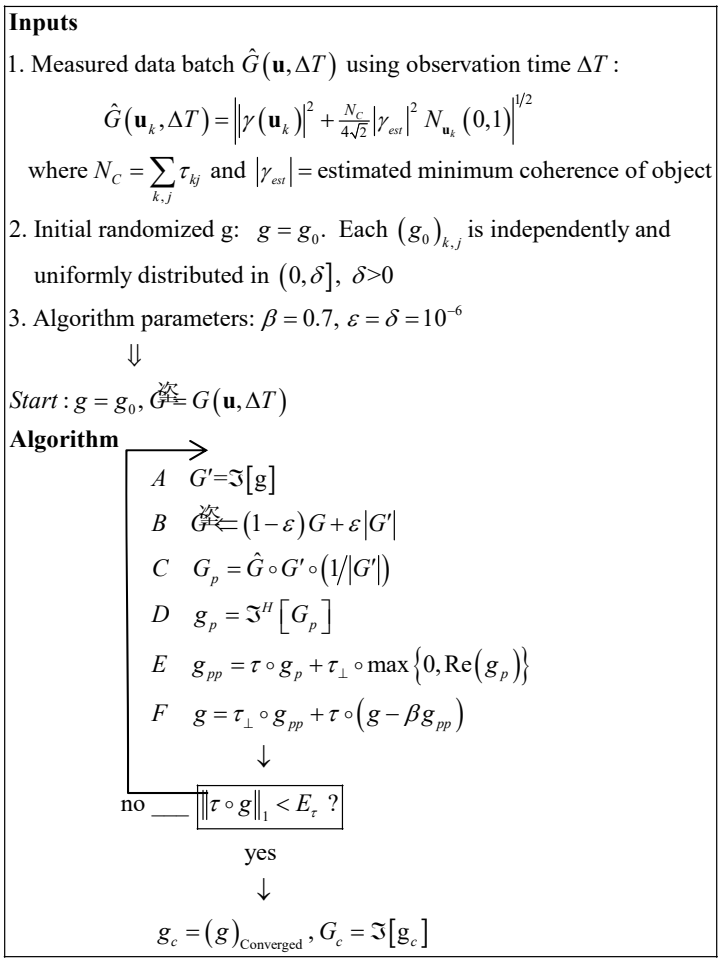

Figure 2. NRPR algorithm as employed in the identification of image constraints.

3. The NRPR Algorithm as a Discrete-Time Dynamic System

As the next step in our analysis, we recast the equations of Figure 2 into a discrete-time dynamic system such that all the principal quantities are indicated by the sequence of integers $k=0,1,...\infty$. We start with the initial conditions and the first iteration and recite the sequence of further iterations, keeping the algorithm in its proper order:

$$\begin{gathered}\hat{G}_{kj}(0)\triangleq\left|\left|\gamma_{kj}\right|^2+\frac{N_C}{4\sqrt{2}}\left|\gamma_{est}\right|^2 N_{kj}(0,1)\right|^{1/2}\\ g(0)=\delta\,rand(N,N),\ \delta=10^{-6}\\ k=0,1,2,...\infty\\ \Downarrow\\ G(k+1)=\Im[g(k)]\\ G \Leftarrow (k+1)=(1-\varepsilon)G(k)+\varepsilon|G(k+1)|\\ \tau\circ g(k+1)=\tau\circ\left\{g(k)-\beta\,\mathrm{Re}\left[\Im^H\left(\hat{G}(k+1)\circ e^{i\arg(G(k+1))}\right)\right]\right\}\\ \tau_\perp\circ g(k+1)=\tau_\perp\circ\mathrm{Re}_+\left[\Im^H\left(\hat{G}(k+1)\circ e^{i\arg(G(k+1))}\right)\right]\end{gathered} \tag{2. a-f}$$

where the function $rand(N,N)$ is an $N\times N$ matrix having statistically independent elements that are uniformly distributed in $[0,1)$. Now consider the equations pertaining to $k=0$ and 1:

 doi:10.20944/preprints202502.1067.v1

$$\hat{G}_{kj}(0) \triangleq \left| \left|\gamma_{kj}\right|^2 + \tfrac{N_C}{4\sqrt{2}} \left|\gamma_{est}\right|^2 N_{kj}(0,1) \right|^{1/2}$$
$$\mathrm{g}(0) = \delta\, rand(N,N),\ \ \delta \cong 10^{-6}$$
$$\Downarrow$$
$$G(1) = \Im\left[\delta\, rand(N,N)\right]$$
$$\hat{G}(1) = (1-\varepsilon)G(0) + \varepsilon\delta \left| e^{i\pi\left[2rand(N,N)-1\right]} \right| = \hat{G}(0) + O(-\varepsilon+\varepsilon\delta)$$
$$\tau \circ g(1) = \tau \circ \left\{ g(0) - \beta\, \mathrm{Re}\left[\Im^H \left(\hat{G}(0) \circ e^{i\pi\left[2rand(N,N)-1\right]} + O(-\varepsilon+\varepsilon\delta) \right) \right] \right\}$$
$$\tau_\perp \circ g(1) = \tau_\perp \circ \mathrm{Re}_+ \left[\Im^H \left(\hat{G}(0) \circ e^{i\pi\left[2rand(N,N)-1\right]} + O(-\varepsilon+\varepsilon\delta) \right) \right]$$

(3.a-d)

Ignoring terms of order ε and $\varepsilon\delta$ these relations become:

$$\hat{G}_{kj}(1) \cong G_{kj}(0) \triangleq \left| \left|\gamma_{kj}\right|^2 + \tfrac{N_C}{4\sqrt{2}} \left|\gamma_{est}\right|^2 N_{kj}(0,1) \right|^{1/2}$$
$$\tau \circ g(1) = \tau \circ \mathrm{Re}\left[\Im^H \left\{ \left[\delta - \beta \hat{G}(0) \right] \circ e^{i\pi\left[2rand(N,N)-1\right]} \right\} \right]$$
$$\tau_\perp \circ g(1) = \tau_\perp \circ \mathrm{Re}_+ \left[\Im^H \left(\hat{G}(0) \circ e^{i\pi\left[2rand(N,N)-1\right]} \right) \right] \qquad \text{(4. a-f)}$$
$$\Downarrow \ \mathrm{k}=1,2,\ldots,\infty$$
$$\hat{G}(k+1) = (1-\varepsilon)G(k) + \varepsilon \left| \Im\left[\mathrm{g}(k) \right] \right|$$
$$\tau \circ g(k+1) = \tau \circ \left\{ g(k) - \beta\, \mathrm{Re}\left[\Im^H \left(\hat{G}(k+1) \circ e^{i\arg\left(\Im\left[\mathrm{g}(k)\right]\right)} \right) \right] \right\}$$
$$\tau_\perp \circ g(k+1) = \tau_\perp \circ \mathrm{Re}_+ \left[\Im^H \left(\hat{G}(k+1) \circ e^{i\arg\left(\Im\left[\mathrm{g}(k)\right]\right)} \right) \right]$$

Regarding the second equation above, $\beta\hat{G}(0)$ is at least three orders of magnitude larger than δ. Thus:

$\left[\delta - \beta \hat{G}(0) \right] \circ e^{i\pi\left[2rand(N,N)-1\right]} \cong -\beta G(0) \circ e^{i\pi\left[2rand(N,N)-1\right]}$. Then the first three equations above are devoid of the very small quantities δ and ε, therefore we have:

$$\hat{G}_{kj}(1) \cong G_{kj}(0) \triangleq \left| \left|\gamma_{kj}\right|^2 + \tfrac{N_C}{4\sqrt{2}} \left|\gamma_{est}\right|^2 N_{kj}(0,1) \right|^{1/2}$$
$$\tau \circ g(1) = -\beta\tau \circ \mathrm{Re}\left[\Im^H \left(\hat{G}(0) \circ e^{i\pi\left[2rand(N,N)-1\right]} \right) \right]$$
$$\tau_\perp \circ g(1) = \tau_\perp \circ \mathrm{Re}_+ \left[\Im^H \left(\hat{G}(0) \circ e^{i\pi\left[2rand(N,N)-1\right]} \right) \right] \qquad \text{(5. a-f)}$$
$$\Downarrow \ \mathrm{k}=1,\ldots,\infty$$
$$\hat{G}(k+1) = (1-\varepsilon)G(k) + \varepsilon \left| \Im\left[\mathrm{g}(k) \right] \right|$$
$$\tau \circ g(k+1) = \tau \circ \left\{ g(k) - \beta\, \mathrm{Re}\left[\Im^H \left(\hat{G}(k+1) \circ e^{i\arg\left(\Im\left[\mathrm{g}(k)\right]\right)} \right) \right] \right\}$$
$$\tau_\perp \circ g(k+1) = \tau_\perp \circ \mathrm{Re}_+ \left[\Im^H \left(\hat{G}(k+1) \circ e^{i\arg\left(\Im\left[\mathrm{g}(k)\right]\right)} \right) \right]$$

This dynamic system replaces six steps per iteration with three steps. Note that the quantity $e^{i\pi\left[2rand(N,N)-1\right]}$ is the phase factor of the Fourier transform of the random initial pixel intensities. The new initial conditions in Equations (5. b-c) are correct to within ε and δ (10^{-6}). This means that to the same small error the complete history of the dynamic system is essentially identical to that of the original NRPR in Figure 2. In particular one must note that (5.b) also leads to the convergence of $\tau \circ g(k)$ to zero as demonstrated in Reference [1] . Therefore in the limit, $\tau_\perp \circ g(k)$ is the ultimate nonnegative dynamic system.

 doi:10.20944/preprints202502.1067.v1

Clearly the phase factor, $e^{i\pi[2rand(N,N)-1]}$, in $\tau \circ g(0)$ and $\tau_{\perp} \circ g(0)$ is a statistical ensemble that encompasses all possible coherence phases. Thus there is a very significant non-zero probability that on any one trial NRPR converges to of the correct coherence phase and magnitude and therefore to the noise-free image.

4. The Stochastic Search Algorithm for Sequential Box Sizes

In this Section we consider the Stochastic Search algorithm employing random coherence phases within the two initial conditions rather than random pixel intensities. Figure 3 shows that the embedded NRPR runs (in blue) use statistically independent and uniformly distributed coherence phases spanning $[-\pi,\pi)$. The search sets up a square "Bx" and runs NRR $n>1$ times until there are two images that are fully correlated. In that case, the two outcomes are the noise-free image (baring 180 degrees of rotation or translations). If there are no such correlations within n computations, then the algorithm reduces the box size and tries again. If by chance a converged image has pixel intensities that reside outside of the box, this indicates that the box is too small to contain the illuminated object, and the box size must be enlarged. Overall this is the process by which the Stochastic Search validates the hypotheses of the box size.

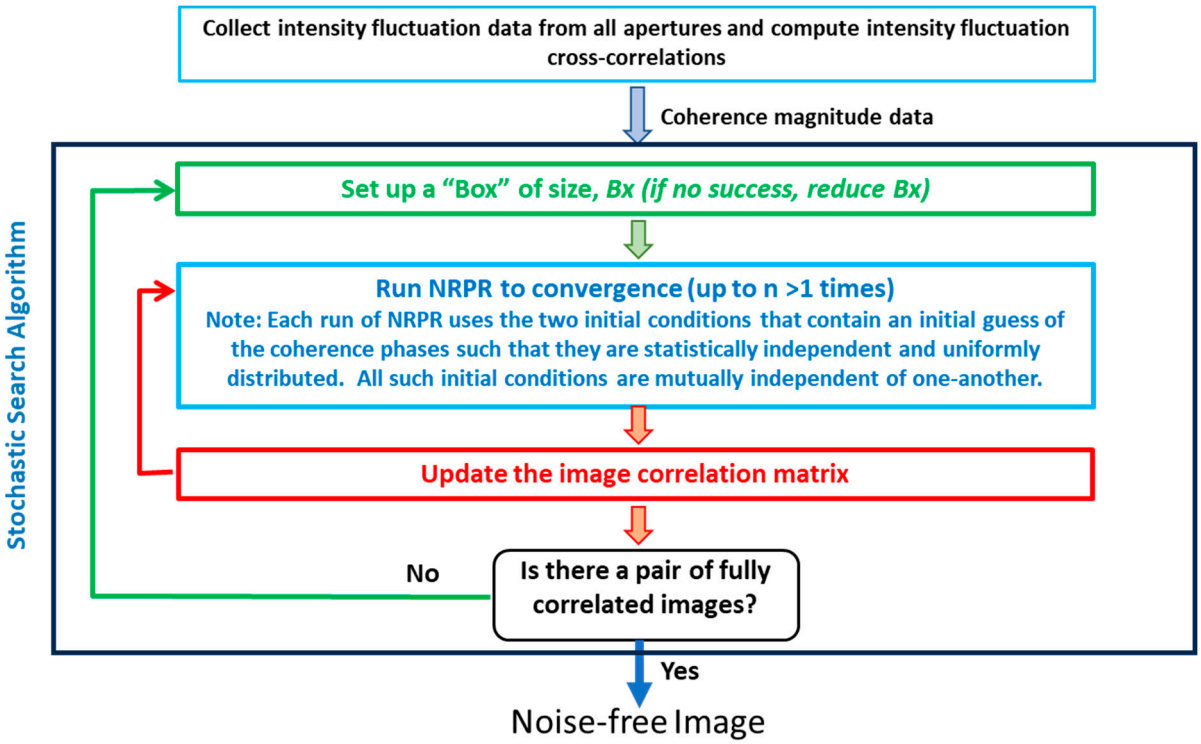

Figure 3. Stochastic Search algorithm using random coherence phases.

In Figure 4 we demonstrate that the dynamic system (5. a-f) behaves essentially as in References [1–3] when in the case that the smallest box size does fully contain the illuminated object. Alternately, one can start with a box size that is smaller than the illuminated object and then increase the box sizes until the noise-free image is found. With this strategy, the number of NRPR computations is distinctly reduced. In fact, if the number of runs is large for the case of decreasing box size, then for the same image, the number of runs for the case of increasing box sizes is halved. The latter strategy, as mentioned in Reference[1] is clearly superior.

Preprints.org (www.preprints.org) | NOT PEER-REVIEWED | Posted: 14 February 2025 doi:10.20944/preprints202502.1067.v1

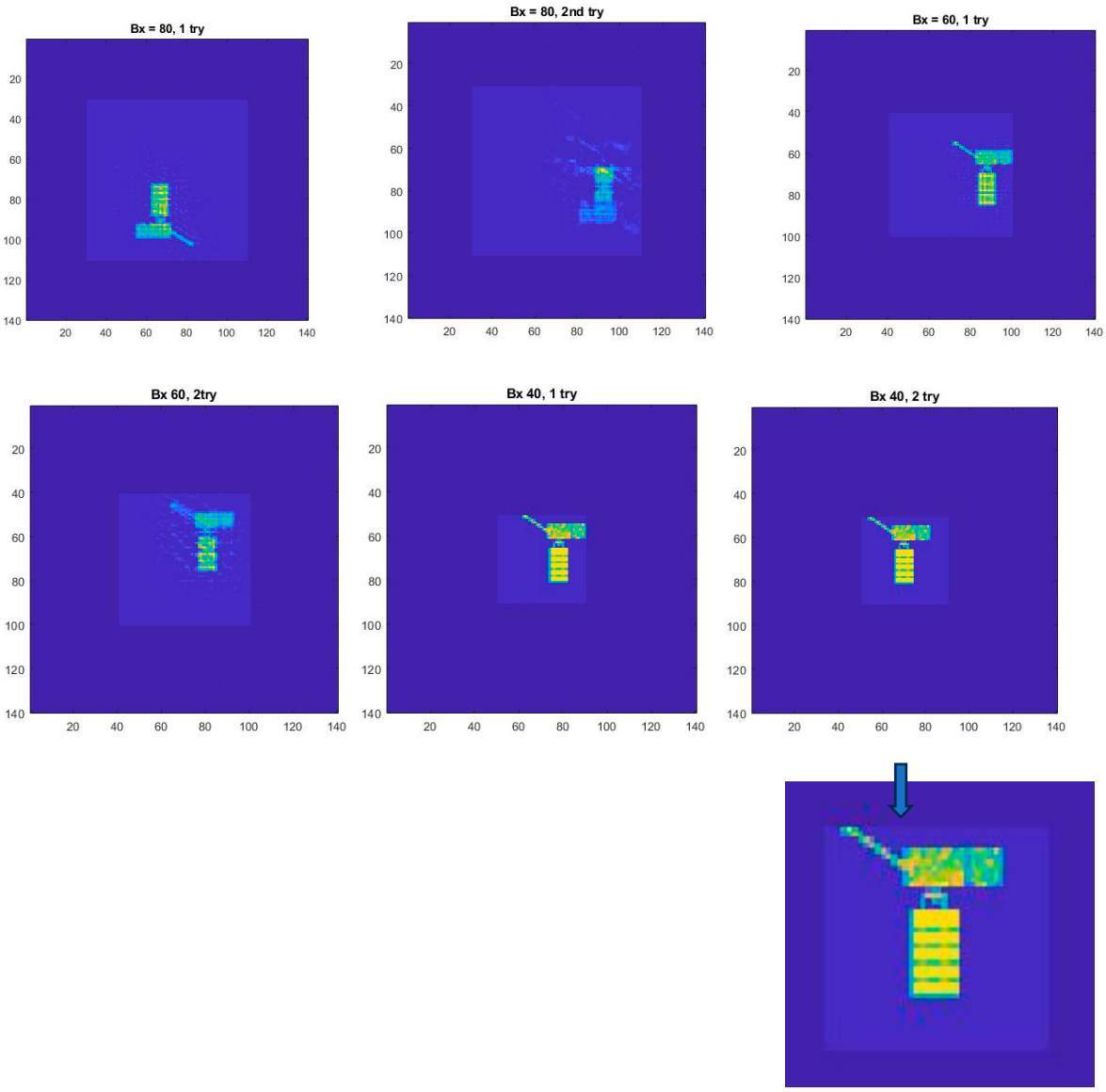

Figure 4. This illustrates how the Stochastic Search uses the nonnegative dynamic system to determine the noise-free image by the regular reduction of the Box size. We start with $B_x = 80$ and run n = 2 trials. Then we then select $B_x = 60$ and $B_x = 40$, each having two trials. The satellite is 50% the size of the 40 pixel box. Consequently we discover that the final pair of images are fully correlated and thus are the noise-free image. The parameters of the dynamic system are $\varepsilon = 10^{-6}$ and $\beta = 0.7$. Each trail was computed for 3000 iterations in approximately 3.5 seconds using an Apexx W Class, thus producing the noise-free image in 21 seconds.

5. Conclusions

Reference [1] created an algorithm that emphatically reduced the integration times of the Brown-Twiss effect as applied to two-dimensional imaging (termed ICI). However, there were a number of complexities in the algorithm that merited simplification. This paper has succeeded in streamlining the ICI algorithm by transforming the six steps of the original algorithm into a discrete-time, nonnegative dynamic system having a three dimensional state space. It is demonstrated that this dynamic system fully replicates the original to within $O(\varepsilon)$. Furthermore, the simplified product, being a nonnegative system [4], is well suited to partner with Artificial Intelligence automation such as nonnegative spiking neural networks. Such automation can be expected in the near future.

The Author is an Independent Researcher.

 doi:10.20944/preprints202502.1067.v1

Supplementary Materials: The following supporting information can be downloaded at the website of this paper posted on Preprints.org.#Reside in the ICI algorithm as described in full detail within the Review.#

Author Contributions: The Author is the sole contributor to the six journal articles under review, including the present one. #

Funding: Aside from the Author's efforts, there are no outside sources of funding for this Review.

Conflicts of Interest: There are no conflicts of interest.

References

1. D. C. Hyland, "Analysis and Refinement of Intensity Correlation Imaging", *Applied Optics,* Vol. 62(21), pp. 5683-5695 (2023).
2. D. C. Hyland, "Improved Integration Time Estimates for Intensity Correlation Imaging", *Applied Optics,* Vol.61, Issue 33, pp. 10002-10011 (2022)
3. D. C. Hyland, "Algorithm for Determination of Image Domain Constraints for Intensity Correlation Imaging", *Applied Optics,* 61(35), pp. 10425-10432 (2022).
4. W. Haddad, V. Chellaboina and Q. Hui, *Nonnegative and Compartmental Dynamical Systems,* Copyright C 2010, Princeton University Press.